Electrochemical Control of the Second Harmonic Generation Property of Self-Assembled Monolayers Containing a *trans*-Ferrocenyl-Nitrophenyl Ethylene Group on Gold

Toshihiro Kondo, Shinya Horiuchi, Ichizo Yagi, Shen Ye, and Kohei Uosaki*

Contribution from the Physical Chemistry Laboratory, Division of Chemistry, Graduate School of Science, Hokkaido University, Sapporo 060-0810, Japan

Received June 8, 1998

Abstract: The second harmonic (SH) intensity at gold electrodes modified with self-assembled monolayers (SAMs) of two novel molecules, which have *trans*-ferrocenyl-nitrophenyl ethylene and thiol groups as the second harmonic generation and surface-attached groups, respectively, was found to be strongly dependent on the oxidation state of the ferrocene group. The SH intensity increased when the ferrocene moiety of the SAMs was oxidized electrochemically to the ferricenium cation, and it decreased and returned to the original value when the ferricenium cation of the ferrocene moiety was reduced to neutral ferrocene. These changes were reversible and were repeated many times. The molecular orientation change in each SAM upon reduction/oxidation of the ferrocene moiety was investigated by in situ Fourier transform infrared reflection−absorption spectroscopy, and the hyperpolarizabilities of these molecules were calculated using a computational electronic structure model. The origin of the SH intensity change is discussed on the basis of these results.

Introduction

Optical second harmonic generation (SHG) is a nonlinear process in which two photons of frequency ω are converted to a single photon of frequency 2ω. This requires a strong electric field and a noncentrosymmetric medium.[1−5] The SHG process is one of the most efficient ways to shorten the wavelength of light. The control of second harmonic (SH) intensity by an external stimulus such as electric and optical perturbation is very important in various applications. One promising system in this respect involves electrochemical control of SH intensity at electrode/electrolyte interfaces. In a metal electrode−electrolyte solution system, the SHG process takes place only at the interface, where centrosymmetry is broken. Because the SH intensity depends on the nonlinear susceptibility of the interface, one should be able to control the SH intensity by controlling the interfacial structure. Although it is known that the SH intensity depends on the electrode potential even at bare metal electrodes,[6−8] a more drastic effect of electrode potential on SH intensity is expected at metal electrodes modified with organic molecules which undergo redox reactions by both molecular hyperpolarizability and molecular orientation, which are known to affect the SH intensity and which are expected to be dependent on the oxidized state of the functional group of the molecule.

To construct a highly efficient SHG-active electrochemical interface, it is essential to arrange a molecule of high molecular polarizability (hyperpolarizability) on the electrode ordered at a molecular level so that high interfacial nonlinear polarizability is attained. The self-assembly (SA) technique has been very widely used to construct ordered molecular layers of various functionalities, and self-assembled monolayers (SAMs) of alkanethiols on gold have been the most well-studied system.[9,10] The molecular layers formed by this method are expected to be very well ordered as a result of the chemical bond formation between the substrate and the sulfur of the thiols and the hydrophobic interaction between alkyl chains. These layers are expected to be more stable than those formed by the LB method because the adsorbed molecules chemisorb on the substrate in the former but physisorb in the latter. Although several reports on SHG from SAM-modified electrodes are available,[11−15] the SHG properties were used to probe the interfacial structure in these studies. For example, Kim et al. measured the rotational anisotropy of the SH intensity from the Au(111) modified with the SAM of 2-mercaptohydroquinone (QSH) to investigate the superlattice structure of the QSH SAM on Au(111).[12] No attempts have been made to construct an electrochemically controllable SHG-active interface by a SAM-based electrode.

(1) Shen, Y. R. *The Principles of Nonlinear Optics*; Wiley: New York, 1994.
(2) Chemla, D. S.; Zyss, J. *Nonlinear Optical Properties of Organic Molecules and Crystals*; Academic Press: New York, 1992.
(3) Eisenthal, K. B. *J. Phys. Chem.* **1996**, *100*, 12997−13006.
(4) Corn, R. M.; Higgins, D. A. *Chem. Rev.* **1994**, *94*, 107−125.
(5) Corn, R. M.; Higgins, D. A. In *Characterization of Organic Thin Films*; Ulman, A., Ed.; Butterworth-Heinemann: New York, 1995.
(6) Bradley, R. A.; Geogiadis, R.; Kevan, S. D.; Richmond, G. L. *J. Chem. Phys.* **1993**, *99*, 5535−5537.
(7) Yagi, I.; Nakabayashi, S.; Uosaki, K. *J. Phys. Chem. B* **1998**, *102*, 2677−2683.
(8) Yagi, I.; Nakabayashi, S.; Uosaki, K. *Surf. Sci.* **1998**, *406*, 1−8.
(9) Ulman, A. *An Introduction to Ultrathin Organic Films from Langmuir−Blodgett to Self-Assembly*; Academic Press: New York, 1991.
(10) Finklea, H. O. In *Electroanalytical Chemistry*; Bard, A. J., Rubinstein, I., Eds.; Marcel Dekker: New York, 1996; Vol. 19.
(11) Buck, M.; Grunze, M.; Eisert, F.; Fischer, J.; Träger, F. *J. Vac. Sci. Technol. A* **1992**, *10*, 926−929.
(12) Kim, S.; Zhao, M.; Scherson, D. A.; Choi, K.-J.; Bae, I. T. *J. Phys. Chem.* **1994**, *98*, 9383−9386.
(13) Kakkar, A. K.; Yitzchaik, S.; Roscoe, S. B.; Kubota, F.; Allan, D. S.; Marks, T. J. *Langmuir* **1993**, *9*, 388−390.
(14) Li, D.-Q.; Swanson, B. I.; Robinson, J. M.; Hoffbauer, M. A. *J. Am. Chem. Soc.* **1993**, *115*, 6975−6980.
(15) Yitzchaik, S.; Roscoe, S. B.; Kakkar, A. K.; Allan, D. S.; Marks, T. J.; Xu, A.; Zhang, T.; Lin, W.; Wong, G. K. *J. Phys. Chem.* **1993**, *97*, 6958−6960.

10.1021/ja982007a CCC: $18.00
Published on Web 12/29/1998

Scheme 1

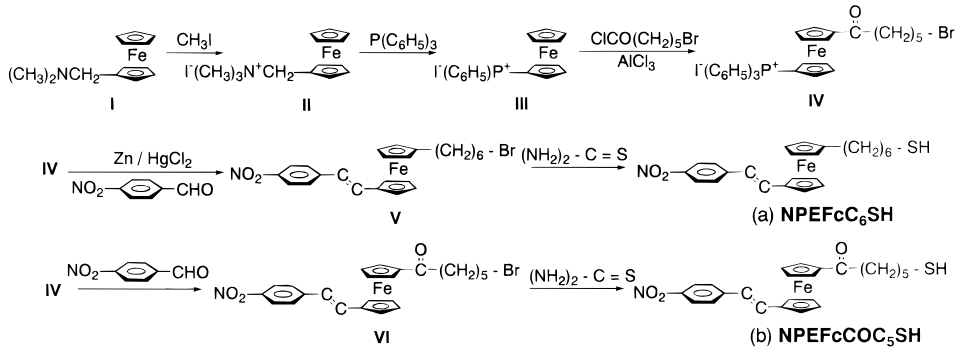

We have already reported on the molecular orientation of the ferrocenylalkanethiol SAM on gold electrodes upon reduction/oxidation of the ferrocene moiety of the SAM.[16−26] It is also known that the *trans*-ferrocenyl-nitrophenyl ethylene group has a high hyperpolarizability, β_{zzz}.[27−30] Thus, an electrode modified with a SAM containing a *trans*-ferrocenyl-nitrophenyl ethylene group should be a good candidate for a stable, efficient, electrochemically controllable system for the SH intensity.

Here we report novel SAM-based systems in which the SH intensity can be controlled electrochemically. The systems consist of gold electrodes modified with the SAM of two novel molecules (*trans*-[1-(6-mercaptohexyl)ferrocenyl-2-(4-nitrophenyl)ethylene] (NPEFcC$_6$SH) and *trans*-[1-(6-mercaptohexanoyl)-ferrocenyl-2-(4-nitrophenyl)ethylene] (NPEFcCOC$_5$SH)), which have both ferrocenyl-nitrophenyl ethylene and thiol groups, as shown in Scheme 1. The SH intensity increased 6 times in the former and 4 times in the latter upon oxidation of the ferrocene moiety of the SAMs. The origin of the SH intensity change is discussed in terms of molecular orientation of the SAMs upon redox of the ferrocene moiety, measured using in situ Fourier transform infrared reflection absorption spectroscopy (FT-IRRAS), and β_{zzz} values of the molecules in the oxidized and reduced states, calculated using a computational electronic structure model of Zerner's intermediate neglect of differential overlap (ZINDO) program.

Theoretical Background

The SHG can be described in terms of the second-order polarization, $P^{(2)}$, induced in the interface by the incident light waves.[2−5] The incident light field $E(\omega)$ at frequency ω generates a light wave at 2ω. The relationship between the induced polarization $P^{(2)}$ and the incident fields is given by

$$P^{(2)}_{(2\omega)} = \chi^{(2)}_{(2\omega)} E(\omega) E(\omega) \tag{1}$$

When a two-dimensional arrangement of adsorbed molecules on the surface is isotropic, the SHG from the monolayer is invariant during rotation of the surface about the surface normal, and the surface nonlinear susceptibility tensor, $\chi^{(2)}$, then has only three unique elements, i.e., χ_{XXZ}, χ_{ZXX}, and χ_{ZZZ}, where the *X* and *Y* axes are surface parallel and the *Z* axis is surface normal. The intensity of p-polarized SH light, $I_p(2\omega)$, can be directly related to these elements:[1−5]

$$I_p(2\omega) \propto |(\mathbf{a}_1\chi_{XXZ} + \mathbf{a}_2\chi_{ZXX} + \mathbf{a}_3\chi_{ZZZ})\cos^2\gamma + \mathbf{a}_4\chi_{ZXX}\sin^2\gamma|^2 I(\omega)^2 \tag{2}$$

where γ and $I(\omega)$ are the polarization angle of the incident light (γ = 0° for p-polarized and 90° for s-polarized light) and the intensity of the incident laser light, respectively. The $\mathbf{a}_i$ terms describe the electric fields in the monolayer and thus include the dielectric constants of the monolayer, $\epsilon(\omega)$ and $\epsilon(2\omega)$.[4,5] When p-polarized incident light is used (γ = 90°), the SH intensity, $I_{pp}(2\omega)$, is simply given by[4,5]

$$I_{pp}(2\omega) \propto |\mathbf{a}_1\chi_{XXZ} + \mathbf{a}_2\chi_{ZXX} + \mathbf{a}_3\chi_{ZZZ}|^2 I(\omega)^2 \tag{3}$$

When the contribution from the substrate is negligible, the elements of $\chi^{(2)}$ can be related only to the elements of the molecular nonlinear polarizability (hyperpolarizability), β, of the adsorbed molecules and the molecular orientation distribution function, *F*. All $\chi^{(2)}$, β, and *F* are presented by the surface coordinate axes, *I*, *J*, and *K*, and the molecular coordinate axes, *i*, *j*, and *k*.[4,5]

$$\chi_{IJK} = \Gamma \sum \langle F_{IJKijk}(\phi,\theta,\alpha)\rangle \beta_{ijk} \tag{4}$$

where Γ is the surface coverage of adsorbed molecules and ϕ, θ, and α are defined relative to the space-fixed molecular coordinates as described in Figure 1.[4,5,31] If β_{zzz} is the only nonzero tensor element, i.e., the molecule has hyperpolarizability only for the *z* direction, then the number of independent surface nonlinear tensor elements is reduced to two:[4,5]

$$\chi_{ZXX} = \chi_{XXZ} = (\Gamma \cos\theta \sin^2\theta\beta_{zzz})/2 \tag{5}$$

$$\chi_{ZZZ} = \Gamma \cos^3\theta\chi_{zzz} \tag{6}$$

and eq 3 is greatly simplified as

$$I_{pp}(2\omega) \propto |\{(\mathbf{a}_1 + \mathbf{a}_2)\sin^2\theta\}/2 + \mathbf{a}_3\cos^2\theta|^2\Gamma^2\cos^2\theta\beta_{zzz}{}^2 I(\omega)^2 \tag{7}$$

When a simple two-level model where the ground (g) and the single excited (n) states are considered (typically a state responsible for an

(16) Uosaki, K.; Sato, Y.; Kita, H. *Langmuir* **1991**, *7*, 1510−1514.
(17) Uosaki, K.; Sato, Y.; Kita, H. *Electrochim. Acta* **1991**, *36*, 1799−1801.
(18) Shimazu, K.; Yagi, I.; Sato, Y.; Uosaki, K. *Langmuir* **1992**, *8*, 1385−1387.
(19) Sato, Y.; Itoigawa, H.; Uosaki, K. *Bull. Chem. Soc. Jpn.* **1993**, *66*, 1032−1037.
(20) Kondo, T.; Takechi, M.; Sato, Y.; Uosaki, K. *J. Electroanal. Chem.* **1995**, *381*, 203−209.
(21) Shogen, S.; Kawasaki, M.; Kondo, T.; Sato, Y.; Uosaki, K. *Appl. Organometallic Chem.* **1992**, *6*, 533−536.
(22) Ohtsuka, T.; Sato, Y.; Uosaki, K. *Langmuir* **1994**, *10*, 3658−3662.
(23) Shimazu, K.; Yagi, I.; Sato, Y.; Uosaki, K. *J. Electroanal. Chem.* **1994**, *372*, 117−124.
(24) Shimazu, K.; Ye, S.; Sato, Y.; Uosaki, K. *J. Electroanal. Chem.* **1994**, *375*, 409−413.
(25) Sato, Y.; Frey, B. L.; Corn, R. M.; Uosaki, K. *Bull. Chem. Soc. Jpn.* **1994**, *67*, 21−25.
(26) Ye, S.; Sato, Y.; Uosaki, K. *Langmuir* **1997**, *13*, 3157−3161.
(27) Laidlaw, W. M.; Denning, R. G.; Verbiest, T.; Chauchard, E.; Persoons, A. *Nature* **1993**, *363*, 58−60.
(28) Calabrese, J. C.; Cheng, L.-T.; Green, J. C.; Marder, S. R.; Tam, W. *J. Am. Chem. Soc.* **1991**, *113*, 7227−7232.
(29) Green, M. L. H.; Marder, S. R.; Thompson, M. E.; Bandy, J. A.; Bloor, D.; Kolinski, P. V.; Jones, R. A. *Nature* **1987**, *330*, 360−362.
(30) Kott, K. L.; Higgins, A.; McMahon, R. J.; Corn, R. M. *J. Am. Chem. Soc.* **1993**, *115*, 5342−5343.
(31) It is noted that molecular coordinates are determined by letting the vector from ferrocene to nitrophenyl group be in the *z* direction.
(32) Kanis, D. R.; Rantner, M. A.; Marks, T. J. *J. Am. Chem. Soc.* **1992**, *114*, 10338−10357.

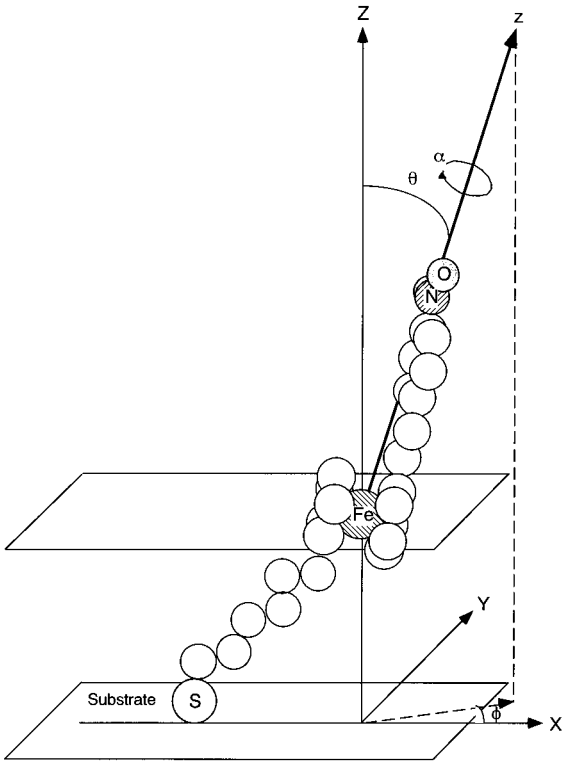

Figure 1. Definition of the angles, α, ϕ, and θ, employed in the molecular orientation calculation. The surface normal and the molecular coordinate are defined as the *Z* and the *z* axes, respectively.

optical transition near the wavelength of interest), the equation for β_{zzz} can be given by[32−34]

$$\beta_{zzz} \propto \frac{f\Delta\mu_{gn}\omega_{gn}}{(\omega_{gn}^2 - 4\omega^2)(\omega_{gn}^2 - \omega^2)} \tag{8}$$

where f, $\Delta\mu_{gn}$, ω_{gn}, and ω are the oscillation strength, the difference in the permanent dipole moment at g, μ_g, and n, μ_n, the excitation frequency from g to n, and the incident laser frequency, respectively. From eqs 7 and 8, to generate a strong SH signal from the monolayer, it is necessary to choose a molecule having high values of f and $\Delta\mu_{gn}$ and having a high resonance of ω_{gn} with ω and/or 2ω, to adsorb many molecules onto the substrate (Γ) and to align the *trans*-ferrocenylnitrophenyl ethylene part of the molecules in one direction (θ).

Results and Discussion

In Situ SHG Measurements. Figure 2 shows the cyclic voltammograms (CVs) and the simultaneously obtained potential dependence of the 1064-nm-excited SHG signal at (a) NPEFcC_6SH, (b) NPEFcCOC_5SH, (c) 6-ferrocenylhexanethiol (FcC_6SH), and (d) hexanethiol (C_6SH) SAM-modified gold electrodes measured in 0.1 M $HClO_4$ solution at a scan rate of 5 mV s^{-1}. Dipping times for the surface modification were 12 h for NPEFcC_6SH and NPEFcCOC_5SH and 1 h for FcC_6SH and C_6SH. The CV and the potential dependence of the SHG signal at a bare gold electrode are also shown in Figure 2e for comparison.

At the NPEFcC_6SH, NPEFcCOC_5SH, and FcC_6SH SAM-modified gold electrodes, anodic and cathodic current peaks due to the reduction/oxidation of the ferrocene moiety in the SAMs were observed at 400 and 410 mV, 640 and 720 mV, and 405 and 415 mV, respectively. The redox potential of the NPEFcCOC_5SH SAM was more positive than those of the NPEFcC_6SH and FcC_6SH SAMs because of the electron-withdrawing effect of the carbonyl group which existed next to the ferrocene ring of NPEFcCOC_5SH.[20,35] The surface coverage, Γ, of the NPEFcC_6SH, NPEFcCOC_5SH, and FcC_6SH SAMs was estimated to be 1.7×10^{14}, 2.0×10^{14}, and 4.0×10^{14} molecules cm^{-2}, respectively, from the redox charge of the ferrocene moiety. The Γ values of the NPEFcC_6SH and NPEFcCOC_5SH SAMs were lower than that of FcC_6SH. This should be due to the effect of the steric hindrance of the nitrophenyl ethylene group.

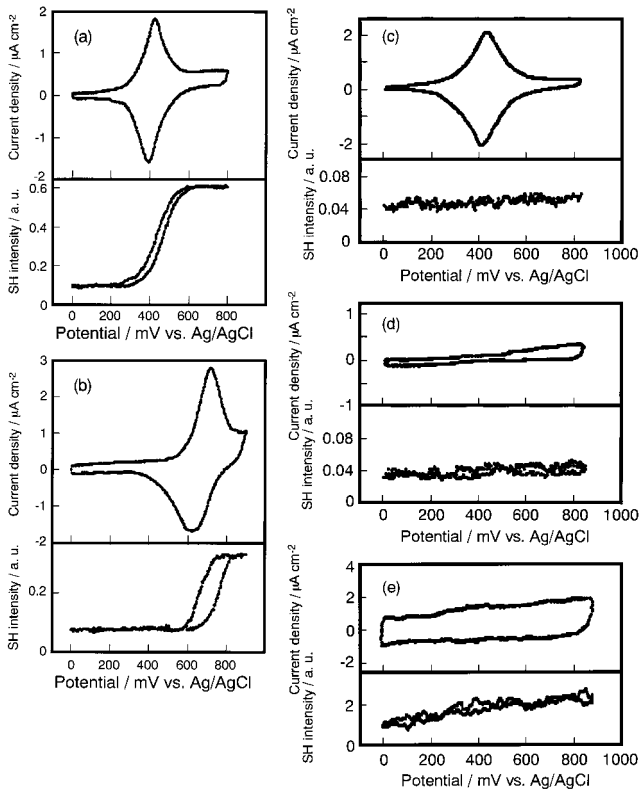

Figure 2. Cyclic voltammograms and potential dependence of 1064-nm-excited SHG (532 nm) at (a) NPEFcC_6SH SAM-modified, (b) NPEFcCOC_5SH SAM-modified, (c) FcC_6SH SAM-modified, (d) C_6-SH SAM-modified, and (e) bare gold electrodes measured in 0.1 M $HClO_4$ solution at a scan rate of 5 mV s^{-1}. The dipping times of the surface modification were 12 h for NPEFcC_6SH and NPEFcCOC_5SH and 1 h for FcC_6SH and C_6SH. The SH intensity was normalized by the intensity from the bare gold at 0 mV, which was measured after thiol molecules were desorbed anodically, and the intensity of the incident light (1064 nm).

Since the gold electrode used in the present study has (111) surface structure, the SH intensity depends on the azimuthal angle. When the SH intensity was measured at an azimuthal angle of 0° at the bare gold electrode, the SH intensity increased linearly with the electrode potential, as shown in Figure 2e.[6,36] At the FcC_6SH SAM-modified and C_6SH SAM-modified gold electrodes (Figure 2c,d), however, the SH intensity was not changed in the potential region employed in the present study at all the azimuthal angles. These results indicate that the adsorption of thiol molecules reduces the contribution of the gold surface to SHG. We also observed that the SH intensity did not depend on potential at all the azimuthal angles at the

(33) Oudar, J. L.; Chemla, D. S. *J. Chem. Phys.* **1977**, *66*, 2664−2668.
(34) Moylan, C. R.; Ermer, S.; Lovejoy, S. M.; McComb, I.-H.; Leung, D. S.; Wortmann, R.; Krdmer, P.; Twieg, R. J. *J. Am. Chem. Soc.* **1996**, *118*, 12950−12955.
(35) Mann, C. K.; Barnes, K. K. *Electrochemical Reactions in Nonaqueous Systems*; Marcel Dekker: New York, 1970.
(36) Yagi, I.; Nakabayashi, S.; Uosaki, K. Manuscript in preparation.

Table 1. SH Intensity[a] at the Bare and Modified Gold Electrodes at 0 and 850 mV

electrodes	SH intensity at 0 mV	SH intensity at 850 mV
bare gold	1.0	2.0
C_6SH SAM	0.04	0.04
FcC_6SH SAM	0.04	0.06
$NPEFcC_6SH$ SAM	0.11	0.61
$NPEFcCOC_5SH$ SAM	0.08	0.33

[a] Values of the SH intensity were normalized to the SH intensity at the bare gold at 0 mV and the intensity of the incident light.

gold surface after sulfur adsorption.[36] Sulfur or thiol adsorption seems to pin the surface electronic structure of gold. Thus, we can neglect the contribution of gold in the potential-dependent SHG behavior at the SAM-modified gold electrode.

At the $NPEFcC_6SH$ and $NPEFcCOC_5SH$ SAM-modified gold electrodes, the SH intensity increased when the potential was made more positive so that the ferrocene moiety was oxidized to the ferricenium cation. It became constant after the oxidation of the ferrocene moiety in the SAMs was completed. When the ferricenium cation was reduced back to the neutral ferrocene, the SH intensity decreased and returned to the original values. These SH intensity changes at the $NPEFcC_6SH$ and $NPEFcCOC_5$-SH SAMs were observed to be reversible.

The SH intensities at 0 and 850 mV for all electrodes studied are summarized in Table 1. At all the SAM-modified gold electrodes, those values were normalized to the values observed at 0 mV after the SAMs were anodically removed from the gold surface in the same solution. The SH intensities at all the SAM-modified gold electrodes at both 0 and 850 mV were much lower than those at the bare gold, indicating that the SAM formation on the gold surface reduced the SH intensity, i.e., the $\chi^{(2)}$ at the gold electrode/electrolyte solution interface.[11,36] Buck et al.[11] have already reported that the intensity of the SH signal decreased with the increase in the coverage of thiols on the gold surface.

The SH intensities at the $NPEFcC_6SH$ and $NPEFcCOC_5SH$ SAM-modified electrodes were larger than those at the FcC_6-SH and C_6SH SAM-modified electrodes at both 0 and 850 mV, indicating higher β_{zzz} values for these molecules.

Although the potential dependence of the SH intensities at the FcC_6SH and C_6SH SAM-modified electrodes and the bare gold was very small, those at the $NPEFcC_6SH$ and $NPEFcCOC_5$-SH SAMs at 850 mV were much larger than those at 0 mV as a result of the oxidation of the ferrocene moiety, as mentioned before.

According to eq 3, the square root of the SH intensity, $I_{pp}(2\omega)^{1/2}$, depends directly on the surface susceptibility. To investigate the relationship between the surface susceptibility and the oxidation state of the ferrocene moiety in the SAMs, the values of $I_{pp}(2\omega)^{1/2}$ were plotted against the oxidation charge at the $NPEFcC_6SH$ and $NPEFcCOC_5SH$ SAM-modified gold electrodes and are shown in Figure 3. The oxidation charge was estimated from the oxidation and reduction peaks in Figure 1 after subtracting the double-layer charging current. In the positive scan (○), $I_{pp}(2\omega)^{1/2}$ continued to increase up to the potential at which the oxidation of the ferrocene moiety in the SAM to ferricenium cation was completed, and then it decreased and returned to the original value in the negative scan (×). These results confirm that the SH intensity change is directly related to the redox of the ferrocene moiety in the SAM. Although no hysteresis was observed at the $NPEFcC_6SH$ SAM-modified electrode, some hysteresis exists in the potential dependence of $I_{pp}(2\omega)^{1/2}$ at the $NPEFcCOC_5SH$ SAM-modified electrode.

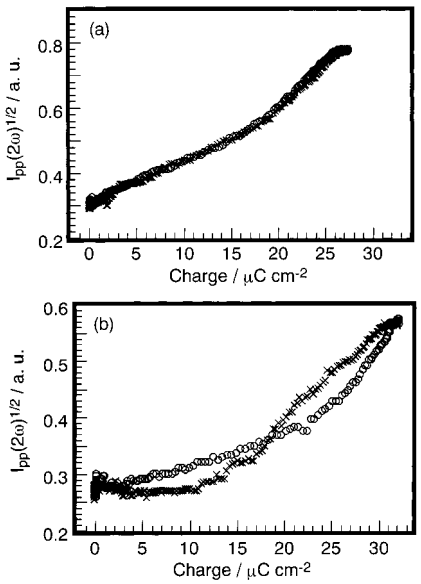

Figure 3. Charge dependence of the square roots of the SH intensity, $I_{pp}(2\omega)^{1/2}$, at (a) $NPEFcC_6SH$ and (b) $NPEFcCOC_5SH$ SAM-modified gold electrodes. Positive and negative scans are represented by ○ and ×, respectively. Other experimental conditions were the same as in Figure 2.

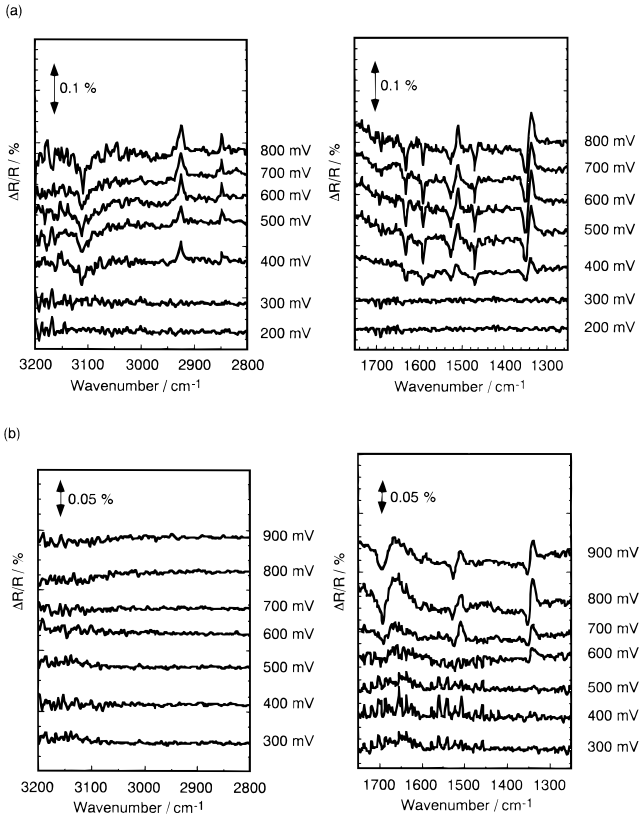

Figure 4. SNIFTIR spectra of (a) $NPEFcC_6SH$ and (b) $NPEFcCOC_5$-SH SAM-modified gold electrodes obtained by p-polarization in 0.1 M $HClO_4$ solution at various sample potentials shown in the figure. The reference potential was 0 V.

In Situ FT-IRRAS Measurements. Figure 4 shows the subtractively normalized interfacial Fourier transform infrared reflection−absorption (SNIFTIR) spectra in the regions of 3200−2800 and 1750−1250 cm^{-1} of the $NPEFcC_6SH$ and $NPEFcCOC_5SH$ SAM-modified gold electrodes obtained at various sample potentials in 0.1 M $HClO_4$ solution with a

reference potential of 0 mV using p-polarized light. Clear peaks exist in both spectra at relatively positive potentials. On the other hand, no bands were observed when the s-polarized light was used, showing that the bands observed in Figure 4 are really due to the attached $NPEFcC_6SH$ and $NPEFcCOC_5SH$ SAMs on the gold substrate.

At the $NPEFcC_6SH$ SAM-modified gold electrode, two upward peaks at 2925 and 2845 cm^{-1} and one downward peak at 3111 cm^{-1} were observed in the region of 3200−2800 cm^{-1} when the sample potential was more positive than +300 mV, at which the redox reaction of the ferrocene moiety in the $NPEFcC_6SH$ SAM started. The two upward peaks at 2925 and 2845 cm^{-1} are attributed to the asymmetric and symmetric C−H stretch, respectively, of the methylene group in the SAM.[37,38] The positions of these two peaks are in good agreement with those observed in ex situ IRRAS spectra of the $NPEFcC_6SH$ SAM on gold (2925 and 2847 cm^{-1}).[25,26,39,40] The downward peak at 3111 cm^{-1} should be due to the C−H stretch of two pentadienyl rings in the ferrocene moiety in the SAM.[41] A similar band at 3113 cm^{-1} was observed for 11-ferrocenylundecanethiol ($FcC_{11}SH$) SAM by in situ IRRAS measurements.[26]

The upward and downward bands in the SNIFTIR spectra indicate weaker and stronger infrared absorption, respectively, at the sample potential than at the reference potential.[37] Thus, the above result shows that the absorptions due to the C−H stretch of the ferrocene ring (3111 cm^{-1}) increased but those due to the asymmetric and symmetric C−H stretch of the methylene groups (2925 and 2845 cm^{-1}, respectively) decreased upon oxidation of the ferrocene group at the $NPEFcC_6SH$ SAM-modified gold electrode. Because p-polarized light was used for this measurement, the stronger the IR absorption is, the more perpendicular to the surface the dipole moment is, according to the "surface selection rule" of IRRAS measurement on a metal surface.[42] Thus, these results show that the alkyl chain of the $NPEFcC_6SH$ SAM became more perpendicular upon oxidation of the ferrocene moiety, as schematically shown in Figure 5a. A similar orientation change was observed at the $FcC_{11}SH$ SAM on a gold electrode.[26]

In the region of 1750−1250 cm^{-1}, three downward peaks at 1630, 1589, and 1468 cm^{-1} were observed when the sample potential was more positive than +300 mV. They were assigned to the C═C stretch of the ethylene group between the ferrocene and nitrophenyl groups, the ring mode of the phenyl group, and the bending mode of the methylene group, respectively.[37,38,41] The increases in absorbance of these bands are in good agreement with the orientation change in the SAM suggested above, based on the C−H stretch. Two other bands of bipolar type were observed around 1512 and 1343 cm^{-1} and were assigned to asymmetric and symmetric NO_2 stretch bands, respectively.[37,38] Bands of bipolar type mean that the frequency of the peak shifts to a higher value upon oxidation of the ferrocene group.[43] The frequency shift should reflect the fact that the electrons in the NO_2 group were attracted electrostatically to the oxidized form of ferrocene, i.e., the ferricenium cation.

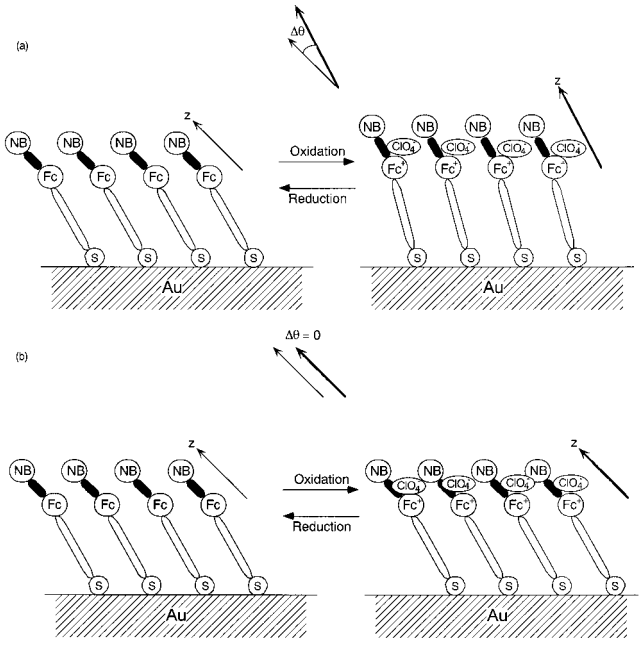

Figure 5. Schematic models for the orientation change in (a) $NPEFcC_6SH$ and (b) $NPEFcCOC_5SH$ SAMs upon redox of the ferrocene moiety. Arrows and $\Delta\theta$ are the vector from ferrocene to nitrophenyl group and the difference angle of those vectors upon the redox of ferrocene, respectively.

In contrast to the result at the $NPEFcC_6SH$ SAM, no bands in the region of 3200−2800 cm^{-1} were observed at the $NPEFcCOC_5SH$ SAM at all the sample potentials studied. In the region of 1750−1250 cm^{-1}, only three bands of bipolar type were observed around 1670, 1512, and 1343 cm^{-1}, which were assigned to C═O, asymmetric NO_2, and symmetric NO_2 stretch bands, respectively,[37,38] when the sample potential was more positive than +500 mV, where the oxidation of the ferrocene moiety in the $NPEFcCOC_5SH$ SAM started. The C═O band of bipolar type indicates the frequency shift as described above. The bipolar band corresponding to the C═O stretch was reported before for the 11-mercaptoundecyl ferrocenecarboxylate ($FcCOOC_{11}SH$) SAM on gold upon reduction/oxidation of the ferrocene moiety in the SAM.[41] No observation of the dominant upward and/or downward peaks in the spectra indicates that the orientation of the $NPEFcCOC_5SH$ SAM did not change during the redox reaction of the ferrocene moiety in the SAM, as shown in Figure 5b.

Calculation of β_{zzz} of the Molecules in Oxidized and Reduced States. The β_{zzz} can be calculated by eq 8 if the values of oscillation strength, f, the difference in the permanent dipole moment between μ_g and μ_n, $\Delta\mu_{gn}$, and the excitation frequency, ω_{gn}, are known. These values were obtained by ZINDO calculation. The values of β_{zzz} as well as f, $\Delta\mu_{gn}$, and ω_{gn} of both the oxidized and reduced states of $NPEFcC_6SH$, $NPEFcCOC_5SH$, and FcC_6SH and a reference compound, *trans*-(1-ferrocenyl)-2-(4-nitrophenyl)ethylene (NPEFc), are listed in Table 2. The values for NPEFc in the reduced state for the incident light of 1.91 μm are also listed in Table 2 for comparison with the literature value.[32]

For all the molecules, the oscillation strength in the oxidized and reduced states are almost the same, showing that the oscillation strength is not affected by the oxidation state of the ferrocene moiety.

(37) Colthup, N. B.; Daly, L. H.; Wiberley, S. E. *Introduction to Infrared and Raman Spectroscopy*, 3rd ed.; Academic Press: New York, 1990.
(38) Silverstein, R. M.; Bassler, G. C.; Morrill, T. C. *Spectrometric Identification of Organic Compounds*, 4th ed.; John Wiley & Sons: New York, 1991.
(39) Porter, M. D.; Bright, T. B.; Allara, D. L.; Chidsey, C. E. D. *J. Am. Chem. Soc.* **1987**, *109*, 3559−3568.
(40) Walczak, M. M.; Chung, C.; Stole, S. M.; Widrig, C. A.; Porter, M. D. *J. Am. Chem. Soc.* **1991**, *113*, 2370−2378.
(41) Popenone, D. D.; Deinhammer, R. S.; Porter, M. D. *Langmuir* **1992**, *8*, 2521−2530.
(42) Greenler, R. G. *J. Chem. Phys.* **1966**, *44*, 310−315.
(43) Beden, B.; Lamy, C. In *Spectroelectrochemistry Theory and Practice*; Gale, R. J., Ed.; Plenum Press: New York, 1988.

Table 2. Calculated Optical Parameters, f, $\Delta\mu_{gn}$, ω_{gn}, and β_{zzz}, in This Study When the Wavelength of the Incident Light and the Second Harmonic Are 1.06 μm and 532 nm, Respectively

molecules	state[a]	f	$\Delta\mu_{gn}$/D	$\omega_{gn}/10^6$ Hz (λ_{max}/nm)	$\beta_{zzz}/10^{-30}$ cm^5 esu^{-1}
NPEFc	R[b]	0.90	8.4	2.82 (354)	71.6
	R	0.91	8.4	2.90 (345)	155
	O	0.89	34.8	3.31 (302)	262
NPEFcC$_6$SH	R	0.98	8.4	2.95 (339)	147
	O	0.87	33.9	3.31 (302)	250
NPEFcCOC$_5$SH	R	1.00	3.9	2.88 (347)	82.3
	O	0.93	15.7	3.16 (316)	164
FcC$_6$SH	R	0.60	0.45	2.48 (404)	25.4
	O	0.75	2.1	3.25 (308)	11.4

[a] R and O mean the reduced and the oxidized states, respectively. [b] These values were calculated when the wavelength of the incident light was 1.91 μm.

The values of $\Delta\mu_{gn}$ in the oxidized states are much larger than those in the reduced states, suggesting that the dipole moment of the excited state increases extensively when the ferrocene moiety is oxidized because of the ion-pair formation between the ferricenium cation and ClO_4^-. The values of $\Delta\mu_{gn}$ for FcC$_6$SH were much smaller than those of other molecules, because no acceptor group, such as a nitrophenyl group, exists in this molecule; therefore, the dipole moment of this molecule is much lower than those of other molecules.

The ω_{gn} value corresponds to the wavelength of the maximum peak in the UV−visible absorption spectrum, λ_{max}. The λ_{max} values for all the molecules calculated in the present study were smaller by 20−30 nm than those experimentally determined using a long optical path length thin-layer electrochemical cell in acetonitrile solution.[44] This is because the solvent effect was not taken into account in the present calculation.[45] The values of ω_{gn} in the oxidized state are larger than those in the reduced state. Actually, the UV absorption peaks corresponding to the π-conjugated system of these molecules blue-shifted in acetonitrile when the ferrocene moiety was oxidized electrochemically.[44]

The β_{zzz} of NPEFc, 71.6 $\times$ 10^{-30} cm^5 esu^{-1}, at 1.91-μm excitation is in good agreement with the literature value (71.8 $\times$ 10^{-30} cm^5 esu^{-1}),[32] showing the reliability of the present calculation. The β_{zzz} values of NPEFc, NPEFcC$_6$SH, and NPEFcCOC$_5$SH in both oxidized and reduced states were much larger than those of FcC$_6$SH in both states, confirming that the NPEFc group has a large hyperpolarizability. This is because π bonding of the ethylene group connects an electron donor, ferrocene, and an electron acceptor, the nitrophenyl group, in the NPEFc group.

For NPEFc, NPEFcC$_6$SH, and NPEFcCOC$_5$SH, the β_{zzz} values in the oxidized states were much larger than those in the reduced states. From eq 8, the larger β_{zzz} should be related to the larger values of $\Delta\mu_{gn}$ in the oxidized states, although the resonance of ω_{gn} with 2ω was smaller in the oxidized states than in the reduced states. Thus, for these molecules, the values of the β_{zzz} are affected by $\Delta\mu_{gn}$ more significantly than by resonance.

Table 3. Square Roots of the SH Intensity ($I_{pp}(2\omega)^{1/2}$) Ratio[a] and the β_{zzz} Ratio[b] between the Reduced and the Oxidized States

molecules	$I_{pp}(2\omega)^{1/2}$ ratio	β_{zzz} ratio
NPEFcC$_6$SH	2.4	1.7
NPEFcCOC$_5$SH	2.0	2.0

[a] $I_{pp}(2\omega)^{1/2}$ ratio means ($I_{pp}(2\omega)^{1/2}$ in the oxidized state)/($I_{pp}(2\omega)^{1/2}$ in the reduced state). [b] β_{zzz} ratio means (β_{zzz} in the oxidized state)/(β_{zzz} in the reduced state).

The β_{zzz} values of NPEFcC$_6$SH were larger than those of NPEFcCOC$_5$SH in both the oxidized and reduced states. This is because the $\Delta\mu_{gn}$ values of NPEFcC$_6$SH in both the oxidized and reduced states were larger than those of NPEFcCOC$_5$SH. Because the C═O group is an electron acceptor group, NPEFcCOC$_5$SH has two acceptor groups at both sides of the donor group, i.e., ferrocene, and, therefore, $\Delta\mu_{gn}$ and β_{zzz} of NPEFcCOC$_5$SH were smaller than those of NPEFcC$_6$SH.

Origin of Redox-Induced SH Intensity Change. According to eq 7, the SH intensity, $I_{pp}(2\omega)$, depends on several parameters, such as molecular hyperpolarizability, β_{zzz}, surface coverage, Γ, and molecular orientation angle, θ. The Γ values are constant upon redox of the ferrocene moiety at both the NPEFcC$_6$SH and NPEFcCOC$_5$SH SAM-modified electrodes because the anodic and cathodic peak charges were the same. Thus, the contribution of the surface coverage to the SH intensity change should be excluded, and β_{zzz} and θ are the dominant factors. To clarify the origin of the SH intensity change at the SAM-modified gold electrodes, we compared the ratio of the square root of the SH intensity, $I_{pp}(2\omega)^{1/2}$, with the ratio of the calculated β_{zzz} between the oxidized and reduced states. If the $I_{pp}(2\omega)^{1/2}$ ratio between the oxidized and reduced states is the same as the ratio of β_{zzz} between the two states, the SH intensity change should be caused solely by the β_{zzz} change, but if the ratio of $I_{pp}(2\omega)^{1/2}$ is larger or smaller than that of β_{zzz}, the contribution of the θ change and the effect of local field on β_{zzz} should be taken into account.

Table 3 shows the ratios of $I_{pp}(2\omega)^{1/2}$ at the NPEFcC$_6$SH and NPEFcCOC$_5$SH SAM-modified electrodes and β_{zzz} of NPEFcC$_6$SH and NPEFcCOC$_5$SH molecules between the oxidized and reduced states. At the NPEFcC$_6$SH SAM-modified electrode, the ratio of $I_{pp}(2\omega)^{1/2}$ was larger than that of β_{zzz}. If local field effect is important, then the discrepancy between the ratio of $I_{pp}(2\omega)^{1/2}$ and that of calculated β_{zzz} should be observed in both cases. Thus, the change in θ seems to contribute to the SH intensity at the NPEFcC$_6$SH SAM-modified gold electrode in addition to the change in β_{zzz}. Actually, in situ IRRAS measurement shows that the alkyl chain of the NPEFcC$_6$SH SAM became more perpendicular upon oxidation of the ferrocene moiety, as mentioned before. When the alkyl chain becomes more perpendicular, θ between the vector from ferrocene to nitrophenyl group and the surface normal should become smaller because the ferrocene ring and the nitrophenyl group are connected through a rigid C═C bond. According to eq 7, the lower θ is, the higher the SH intensity becomes. Thus, the change in θ also contributes to the increase in $I_{pp}(2\omega)$ at the NPEFcC$_6$SH SAM-modified gold electrode upon oxidation of the ferrocene moiety, leading to the increase in $I_{pp}(2\omega)$ being more than expected on the basis of the increase of the β_{zzz} of the molecule.

On the other hand, at the NPEFcCOC$_5$SH SAM-modified electrode, the ratio of $I_{pp}(2\omega)^{1/2}$ is exactly the same as that of β_{zzz}, showing that the dominant contributor to the SH intensity

(44) Kondo, T.; Horiuchi, S.; Uosaki, K.; Shimazu, K. Unpublished results.

(45) Campbell, D. J.; Higgins, D. A.; Corn, R. M. *J. Phys. Chem.* **1990**, *94*, 3681−3689.

change should be β_{zzz}. This is in agreement with the experimental result obtained by in situ IRRAS measurement in which no molecular orientation change took place during the reduction/oxidation of the ferrocene moiety at the $NPEFcCOC_5SH$ SAM-modified gold electrode.

Conclusions

Electrochemically controllable SHG-active SAMs were constructed on gold using molecules having a *trans*-(1-ferrocenyl)-2-(4-nitrophenyl)ethylene group. The SH intensity increased when the ferrocene moiety was oxidized to the ferricenium cation and became constant after the oxidation of the ferrocene moiety in the SAMs was completed. When the ferricenium cation was reduced back to the neutral ferrocene, the SH intensity decreased and returned to the original value. These SH intensity changes were reversible and can be repeated many times. The origin of the SH intensity change was found to be the changes in orientation of the SAM and of the hyperpolarizabilities of these molecules.

Experimental Section

Materials. All the chemicals used in this study were of reagent grade. They were obtained from Aldrich ($CDCl_3$), Tokyo Kasei (6-bromohexanoyl chloride and *N*,*N*-dimethylaminomethyl ferrocene (**I** in Scheme 1)), Merck ($AlCl_3$), and Wako Chemicals (all other chemicals) and were used as received. Ultrapure water was obtained using a Milli-Q water purification system (Yamato, WQ-500). A gold disk (Ishihuku Metal, 99.99%; diameter, 8 or 10 mm; thickness, 5 mm) was used as a substrate. Ultrapure N_2 (99.99%) and Ar (99.95%) were obtained from Daido Hokusan.

Synthetic Procedures. Synthetic routes for *trans*-[1-(6-mercaptohexyl)ferrocenyl-2-(4-nitrophenyl)ethylene] (**$NPEFcC_6SH$**) and *trans*-[1-(6-mercaptohexanoyl)-ferrocenyl-2-(4-nitrophenyl)ethylene] (**$NPEFcCOC_5SH$**) are shown in Scheme 1. 6-Ferrocenylhexanethiol (**FcC_6SH**), (ferrocenyl)trimethylammonium iodide (**II**), (ferrocenyl)triphenylphosphonium iodide (**III**), and *trans*-(1-ferrocenyl)-2-(4-nitrophenyl)ethylene (**NPEFc**) were synthesized using the methods reported before.[16,46,47]

((6-Bromohexanoyl)ferrocenylmethyl)triphenylphosphonium Iodide (IV). **III** (1.0 g, 1.7 mmol) was added to 120 mL of dichloromethane at 0 °C under an Ar atmosphere. After the solution was stirred for 10 min, $AlCl_3$ (0.35 g, 2.6 mmol) was added to the solution, and then 6-bromohexanoyl chloride (0.37 g, 0.7 mmol) was dropped into the solution slowly. The solution was stirred for 3 h at 0 °C. After 150 mL of ice water was added to the solution, the product was extracted with dichloromethane, and the extract was washed with water and evaporated in vacuo overnight. The residue was purified by column chromatography (chloroform) to yield 0.50 g (90% yield) of **IV**. ^{1}H NMR (Hitachi, R-900, 90 MHz, $CDCl_3$): δ 7.68 (d, 15H), 4.90 (t, 4H), 4.29 (d, 2H), 4.03 (d, 4H), 3.36 (t, 2H), 2.75 (t, 2H), 1.56 (m, 6H).

***trans*-[1-(6-Bromohexyl)ferrocenyl-2-(4-nitrophenyl)ethylene] (V).** Zinc amalgam was made by mixing zinc powder (32.8 g, 0.5 mol) with $HgCl_2$ (3.3 g, 0.015 mol) in a solution of HCl (18 mL) and water (48 mL). The zinc amalgam was added slowly to a solution of HCl (50 mL) and water (20 mL) at 60 °C with vigorous stirring, and then an ethanol solution (5 mL) containing **IV** (3.1 g, 4.2 mmol) was added to the solution. The solution was refluxed for 1 h. The product was extracted with dichloromethane, and the extract was evaporated in vacuo overnight. The residue was purified by column chromatography (chloroform) to yield 1.8 g (58% yield) of ((6-bromohexyl)ferrocenylmethyl)triphenylphosphonium iodide. ^{1}H NMR: δ 7.68 (m, 15H), 4.95 (m, 2H), 4.20 (m, 4H), 3.95 (m, 4H), 3.36 (t, 2H), 2.35 (t, 2H), 1.56 (m, 8H). ((6-Bromohexyl)ferrocenylmethyl)triphenylphosphonium iodide (1.8 g, 2.4 mmol) was then added to 20 mL of dioxane under an Ar atmosphere, and the solution was stirred for 10 min. An aqueous solution (2 mL) containing K_2CO_3 (1 g, 4.1 mmol) was dropped into the solution slowly. The solution was refluxed for 4 h after addition of 4-nitrobenzaldehyde (0.74 g, 4.9 mmol). The product was purified by column chromatography (chloroform) to yield 0.45 g (10% yield) of **V**. ^{1}H NMR: δ 8.17 (d, 2H), 7.56 (d, 2H), 6.92 (d, 1H), 6.76 (d, 1H), 4.39 (m, 4H), 4.12 (s, 4H), 3.49 (t, 2H), 2.39 (t, 2H), 1.62 (m, 8H).

***trans*-[1-(6-Mercaptohexanoyl)ferrocenyl-2-(4-nitrophenyl)ethylene] (NPEFcC$_6$SH).** Thiourea (0.15 g, 2.0 mmol) was added to ethanol (10 mL) and water (1 mL) at 80 °C under an Ar atmosphere. **V** (0.45 g, 0.91 mmol) was added to the solution after 5 min, and the solution was stirred for 22 h. The solution was cooled to room temperature, and an aqueous solution (5 mL) containing KOH (0.44 g, 5.6 mmol) was added. The solution was then refluxed for 2 h. The product was extracted with dichloromethane and the extract was washed with water until the pH of the water phase became ca. 7; the extract was then evaporated in vacuo overnight. The residue was purified by column chromatography (ethyl acetate:hexane = 1:1) to yield 0.13 g (32% yield) of **$NPEFcC_6SH$**. ^{1}H NMR: δ 8.18 (d, 2H), 7.55 (d, 2H), 6.95 (d, 1H), 6.75 (d, 1H), 4.40 (m, 4H), 4.10 (m, 4H), 2.60 (t, 2H), 2.25 (t, 2H), 1.60 (m, 9H). IR (neat): 3097, 2925, 2847, 2555, 1628, 1588, 1510, 1456, 1411, 1335 cm^{-1}.

***trans*-[1-(6-Bromohexanoyl)ferrocenyl-2-(4-nitrophenyl)ethylene] (VI).** **IV** (0.50 g, 0.77 mmol) was added to 15 mL of dioxane under an Ar atmosphere, and the solution was stirred for 10 min. An aqueous solution (1 mL) containing K_2CO_3 (0.58 g, 4.1 mmol) was dropped slowly into the solution. 4-Nitrobenzaldehyde (0.35 g, 2.3 mmol) was added to the solution, and then the solution was refluxed for 4 h. The product was purified by column chromatography (chloroform) to yield 0.08 g (20% yield) of **VI**. ^{1}H NMR: δ 8.16 (d, 2H), 7.59 (d, 2H), 6.87 (d, 1H), 6.77 (d, 1H), 4.76 (t, 2H), 4.45 (m, 6H), 3.47 (t, 2H), 2.59 (t, 2H), 1.50 (m, 6H).

***trans*-[1-(6-Mercaptohexanoyl)ferrocenyl-2-(4-nitrophenyl)ethylene] (NPEFcCOC$_5$SH).** Thiourea (0.025 g, 0.33 mmol) was added to 5.5 mL of ethanol and water (10:1) at 80 °C under an Ar atmosphere. **VI** (0.11 g, 0.22 mmol) was added to the solution after 5 min, and the solution was stirred for 22 h. The solution was cooled to room temperature, and an aqueous solution (2 mL) containing KOH (0.11 g, 1.4 mmol) was added. The solution was then refluxed for 2 h. The product was extracted with dichloromethane, and the extract was washed with water until the pH of the water phase became ca. 7; the extract was then evaporated in vacuo overnight. The residue was purified by column chromatography (ethyl acetate:hexane = 1:1) to yield 0.04 g (40% yield) of **$NPEFcCOC_5SH$**. ^{1}H NMR: δ 8.14 (d, 2H), 7.60 (d, 2H), 6.90 (d, 1H), 6.77 (d, 1H), 4.77 (t, 2H), 4.46 (m, 6H), 2.60 (m, 4H), 1.55 (m, 7H). IR (neat): 3096, 2924, 2851, 2554, 1671, 1628, 1588, 1510, 1456, 1411, 1336 cm^{-1}.

Preparation of SAM-Modified Gold Substrate. A gold disk was polished mechanically with alumina paste (Maruto, 1.0, 0.3, and 0.05 μm) and cleaned chemically by dipping in boiling concentrated HNO_3 for 1 h and then in boiling 2 M KOH solution for 2 h.[48,49] The disk was then treated electrochemically by cycling the potential between +1.5 and −0.34 V (vs Ag/AgCl) in 1 M H_2SO_4.[50,51] After these treatments, gold was vacuum deposited (1500 Å) onto the gold disk, which was kept at 300 °C in a vacuum evaporation apparatus (Ulvac, EBH-6) under 10^{-6}−10^{-7} Torr at a deposition rate of 0.1 Å s^{-1}. The gold disk was then annealed at 850 °C for 5 h under an Ar atmosphere and was kept in concentrated H_2SO_4 until the substrate was used for surface modification. The gold surface prepared as described above was atomically flat, with a (111) ordered structure.[52] The roughness factor of the surface was estimated from the charge for the reduction of gold oxide to be less than 1.1. Just before the surface modification,

(46) Pauson, P. L.; Watts, W. E. *J. Chem. Soc.* **1963**, 2990−2996.
(47) Toma, S.; Gáplovsky, A.; Elecko, P. *Chem. Papers* **1985**, *39*, 115−124.
(48) Katz, E. Y.; Solov'ev, A. A. *J. Electroanal. Chem.* **1990**, *291*, 171−186.
(49) Adzic, R.; Yeager, E.; Cahan, B. D. *J. Electrochem. Soc.* **1974**, *121*, 474−484.
(50) Woods, R. In *Electroanalytical Chemistry: A Series of Advances*; Bard, A. J., Ed.; Marcel Dekker: New York, 1988; Vol. 9, pp 1−162.
(51) Rodriguez, J. F.; Mebrahtu, T.; Soriaga, M. P. *J. Electroanal. Chem.* **1987**, *233*, 283−289.
(52) Uosaki, K.; Ye, S.; Kondo, T. *J. Phys. Chem.* **1995**, *99*, 14117−14122.

the gold was washed with pure water and then was annealed in a hydrogen flame and quenched with pure water.

The surface modification of the gold disk substrate was carried out by dipping it in ethanol solution containing 1 mM $NPEFcC_6SH$ or $NPEFcCOC_5SH$ at 20 °C for 12 h and in hexane solution containing 1 mM FcC_6SH or C_6SH for 1 h under an Ar atmosphere. After the modification, the samples were washed sequentially with ethanol or hexane and pure water.

In Situ SHG Measurements.[7,8,53−55] Five nanosecond pulses of fundamental light (1064 nm) generated by a 20-Hz Q-switched Nd:YAG laser (Coherent, Infinity 40-100) were directed onto the SAM-modified gold electrode at a 40° angle of incidence in a single-window spectroelectrochemical cell, which was mounted on an *x*, *y*, *z*, and θ translation stage to allow the placement of the electrode. A slide glass was placed in front of the sample so that roughly 10% of the fundamental beam was reflected into a reference channel. The p-polarization of the fundamental beam was set with a double Fresnel rhomb (Sigma Koki) and a Glan-laser polarizer (Newport). The energy of the pulses was measured by using a broadband power/energy meter (Melles Griot, 13PEM001). The SH light (532 nm), which was almost coincident with the reflected fundamental beam, was collimated by a quartz lens (Sigma Koki). A second Glan-laser polarizer (CVI) was inserted for selection of the SH polarization. The detection system consisted of a small monochromator (Koken, SG-100), a photomultiplier tube (PMT, Hamamatsu, R636-10), and a boxcar averager (Stanford Research, SR250). The PMT voltage was set to 1000 V by a PMT high-voltage supply (Hamamatsu, C1053-01). The output signal was amplified to a detectable level and was monitored by a digitizing oscilloscope (Hewlett-Packard, HP54510B). The width of the boxcar gate was set to about 50% of the width of the output pulse from the PMT. Another boxcar averager was used to integrate the pulse train to obtain the reference intensity. The integrated SH signal was normalized by dividing by the integrated reference output over 30 laser shots.

For spectroelectrochemical measurements, the electrode potential, current, and normalized SH intensity were captured digitally via a computer interface module (Stanford Research, SR245) and a GP-IB board (NEC, PC-9801-29n) and stored on a personal computer. A digital delay generator (Stanford Research, DG-535) was used to generate all the trigger signals to the laser, the detection system, and the computer interfaces and to control the timing of the measurements. The SH intensity from the SAM-modified gold electrode was normalized by that from a bare gold electrode when the SAM was anodically removed in the same electrolyte solution.

In Situ FT-IRRAS Measurements.[19,26,56] In situ FT-IRRAS measurements were performed using a Bio-Rad FTS30 spectrometer equipped with a HgCdTe detector cooled with liquid nitrogen. A spectroelectrochemical cell was employed which allows the electrode to be pushed with a micrometer to the CaF_2 infrared window without rotation of the electrode. The incident angle was ca. 65°, and p-polarized incident light was used. The SNIFTIR spectroscopy method was used to improve the S/N ratio. The spectra were collected at the sample and reference potentials for 128 scans four times with a resolution of 4 cm^{-1}. The reference potential was 0 V in this study. Collection of the spectra was usually started 5 s after the potential was changed. The results are presented in the form of the normalized change in reflectance, i.e., $\Delta R/R$, which is equal to $(R_s - R_r)/R_s$, where R_s and R_r are the reflectance at the sample and the reference potential, respectively. The upward and downward peaks in the spectra respectively mean weaker and stronger absorption at the sample potential compared to that at the reference potential. The potential steps were provided by a personal computer via a 12-bit D/A converter, and the FT-IR spectrometer was controlled by the same computer through a RS-232C interface.

Calculation of β. ZINDO (Sony Tektronix, CAChe system) is a package which consists of intermediate neglect of differential overlap (INDO),[57] INDO for spectroscopy (INDO/S),[58] complete neglect of differential overlap (CNDO),[59] and other computational calculation methods, such as the Pariser−Parr−Pople (PPP) method.[60,61] ZINDO even contains the parameters of the transition metals, e.g., Fe, and, therefore, it can be used for the calculation of properties of complex molecules containing transition metals, e.g., absorption of ferrocene derivatives.[62] By ZINDO calculation, the oscillation strength, *f*, the permanent dipole moments of the ground and excited states, μ_g and μ_n, respectively, and the excitation frequency, ω_{gn}, were obtained in both the oxidized and reduced states of $NPEFcC_6SH$ and $NPEFcCOC_5SH$ when the wavelength of the incident light was 1064 nm. Calculation of the optimized geometry was repeated at least five times to check the reproducibility. When the geometries were calculated for the oxidized states of the ferrocene moiety, ion-pair formation of ferricenium cation−ClO_4^- was considered, and ClO_4^- was placed in close vicinity to the ferrocene ring. The values of β_{zzz} were obtained by using eq 8. The β_{zzz} values of the reference compounds (NPEFc and FcC_6SH) were also obtained.

Acknowledgment. This work was partially supported by Grants-in-Aid for Scientific Research on Priority Area of Electrochemistry of Ordered Interfaces (Nos. 09237101). I.Y. acknowledges the Japan Society for the Promotion of Science for the JSPS Research Fellowships for Young Scientists.

JA982007A

(53) Yagi, I.; Nakabayashi, S.; Uosaki, K. *Chem. Lett.* **1996**, 529−530.
(54) Nakabayashi, S.; Sugiyama, N.; Yagi, I.; Uosaki, K. *Chem. Phys.* **1996**, *205*, 269−275.
(55) Yagi, I.; Lantz, J. M.; Nakabayashi, S.; Corn, R. M.; Uosaki, K. *J. Electroanal. Chem.* **1996**, *401*, 95−101.
(56) Ye, S.; Yashiro, A.; Sato, Y.; Uosaki, K. *J. Chem. Soc., Faraday Trans.* **1996**, *92*, 3813−3812.
(57) Pople, J. A.; Beveridge, D. L.; Dobosh, P. A. *J. Chem. Phys.* **1967**, *47*, 2026−2033.
(58) Ridley, J.; Zenner, M. C. *Theor. Chim. Acta* **1973**, *32*, 111−134.
(59) Pople, J. A.; Segal, G. A. *J. Chem. Phys.* **1965**, *43*, S136−S151.
(60) Pariser, R.; Parr, R. G. *J. Chem. Phys.* **1953**, *21*, 466−471.
(61) Pople, J. A. *Trans. Faraday Soc.* **1953**, *49*, 1375−1385.
(62) Zenner, M. C.; Loew, G. H.; Kirchner, R. F.; Mueller-Westehoff, U. T. *J. Am. Chem. Soc.* **1980**, *102*, 589−600.